BIOCHEMISTRY
including biophysical chemistry & molecular biology

Article

pubs.acs.org/biochemistry

Alzheimer's Disease Amyloid β-Protein Mutations and Deletions That Define Neuronal Binding/Internalization as Early Stage Nonfibrillar/Fibrillar Aggregates and Late Stage Fibrils

Joseph F. Poduslo,*[,†] Kyle G. Howell,[†] Nicole C. Olson,[†,§] Marina Ramirez-Alvarado,[†] and Karunya K. Kandimalla[†,‡]

[†]Departments of Neurology, Neuroscience, and Biochemistry/Molecular Biology, Mayo Clinic, Rochester, Minnesota 55905, United States

[‡]Department of Pharmaceutics, College of Pharmacy, University of Minnesota, Minneapolis, Minnesota 55455, United States

ABSTRACT: Accumulation of amyloid β-protein (Aβ) in neurons has been demonstrated to precede its formation as amyloid plaques in the extracellular space in Alzheimer's disease (AD) patients. Consequently, intraneuronal Aβ accumulation is thought to be a critical first step in the fatal cascade of events that leads to neuronal degeneration in AD. Understanding the structural basis of neuronal binding and uptake of Aβ might lead to potential therapeutic targets that could block this binding and the subsequent neurodegeneration that leads to the pathogenesis of AD. Previously, we demonstrated that mutation of the two adjacent histidine residues of Aβ40 (H13,14G) resulted in a significant decrease in its level of binding to PC12 cells and mouse cortical/hippocampal neurons. We now demonstrate that the weakened neuronal binding follows the mutation order of H13G < H14G < H13,14G, which suggests that the primary domain for neuronal binding of Aβ40 involves histidine at position 13. A novel APP mutation (E693Δ) that produced a variant Aβ lacking glutamate 22 (E22Δ) in Japanese pedigrees was recently identified to have AD-type dementia without amyloid plaque formation but with extensive intraneuronal Aβ in transfected cells and transgenic mice expressing this deletion. Deletion of glutamate 22 of Aβ40 resulted in a 6-fold enhancement of PC12 neuronal binding that was not decreased by the H13G mutation. The dose-dependent enhanced binding of E22Δ explains the high level of intraneuronal Aβ seen in this pedigree. Fluorescence anisotropy experiments at room temperature showed very rapid aggregation with increased tyrosine rigidity of Aβ39E22Δ, Aβ41E22Δ, and Aβ42 but not Aβ40. This rigidity was decreased but not eliminated by prior treatment with dimethyl sulfoxide. Surprisingly, all peptides showed an aggregated state when evaluated by transmission electron microscopy, with Aβ39E22Δ having early stage fibrils, which was also verified by atomic force microscopy. This aggregation was not affected by centrifugation or pretreatment with organic solvents. The enhanced neuronal binding of Aβ, therefore, results from aggregate binding to neurons, which requires H13 for Aβ40 but not for E22Δ or Aβ42. These latter proteins display increased tyrosine rigidity that likely masks the H13 residue, or alternatively, the H13 residue is not required for neuronal binding of these proteins as it is for Aβ40. Late state fibrils also showed enhanced neuronal binding for E22Δ but not Aβ40 with subsequent intraneuronal accumulation in lysosomes. This suggests that there are multiple pathways of binding/internalization for the different Aβ proteins and their aggregation states or fibrillar structure.

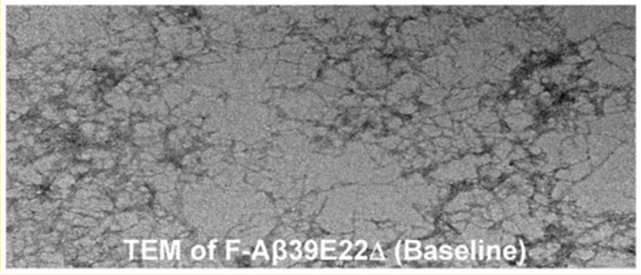

Accumulation of amyloid β-protein (Aβ) in neurons has been demonstrated to precede its formation as amyloid plaques in the extracellular space; consequently, it has been hypothesized that intraneuronal Aβ accumulation is the primary event in the fatal cascade leading to neurodegeneration in Alzheimer's disease (AD) (reviewed in refs 1−5). Recently, we reported that fluorescein-labeled Aβ40 accumulated in PC12 cells and in a subpopulation of cortical and hippocampal neurons through a nonsaturable, energy-independent, non-endocytic pathway with a mechanism involving biophysical interaction with the neuronal membrane.[6] A portion of the internalized Aβ40 was cycled through the endosomes and lysosomes, but a noticeable portion also accumulated outside of these acidic compartments where ultimately it can lead to the degeneration of the neuron.

We have hypothesized that the structural basis for Aβ40 neuronal binding involves a specific domain on Aβ.[7] Indeed, substitution of the two adjacent histidine residues of Aβ40 resulted in a significant decrease in its level of binding with PC12 cells and mouse cortical/hypocampal neurons.[7] In this study, we further delineated the role of these histidine residues in defining the primary domain for neuronal binding of Aβ40.

Received: February 28, 2012
Revised: April 27, 2012
Published: April 30, 2012

Of particular interest is the new Aβ variant lacking glutamate 22 (AβE22Δ) found in a Japanese pedigree having Alzheimer's-type dementia with little amyloid deposition in the patient's brain.[8] Cells transfected with this deletion ($APP_{E693\Delta}$) promoted intracellular accumulation.[9] In addition, APP transgenic mice expressing the E693Δ deletion displayed age-dependent accumulation of intraneuronal Aβ from 8 months, but no extracellular amyloid deposits at 24 months.[10] Because of this intraneuronal accumulation of this Aβ deletion, we hypothesized that this deletion would result in an increased level of binding to PC12 cells compared to that of Aβ40 and questioned whether this binding would be affected by the histidine substitutions as it is for Aβ40.

Further investigations of this Japanese deletion of Aβ protein are not without controversy. The original studies of Tomiyama et al.[8] reported that synthetic Aβ39E22Δ favored oligomer formation but did not form amyloid fibrils. This conclusion was based on negative Pittsburgh B PET scans of patients, the absence of thioflavin-T fluorescence, and the absence of fibrils following electron microscopy. In contrast, Ovchinnikova et al.[11] reported that recombinant Aβ39E22Δ had an increased level of thioflavin-T binding and a strong tendency to form fibrillar bundles. Furthermore, Cloe et al.[12] reported that this deletion has weaker thioflavin-T fluorescence enhancement than Aβ40, forms fibrils instantaneously on the basis of electron microscopy and fluorescence depolarization studies, and does not form oligomers on the basis of size-exclusion chromatography.

These conflicting results likely arise from the starting conformation and assembly state of the Aβ protein. Every laboratory seems to have their preferred procedure for preparing the peptide that varies from treatment with organic solvents, including trifluoroacetic acid (TFA), hexafluoro-2-propanol (HFIP), and dimethyl sulfoxide (DMSO) to treatment with bases (NaOH and NH_4OH) to centrifugation at low or high speeds. If Aβ39E22Δ forms fibrils instantaneously, then ultracentrifugation at 135500*g* would likely remove the fibrils.[11] An approach that we advocate is to minimize harsh treatment of the peptide that might significantly alter its structural state. In any case, we further evaluated these different Aβ peptides by fluorescence anisotropy with and without DMSO treatment, by transmission electron microscopy time course studies with or without DMSO or HFIP treatment, by atomic force microscopy, and by centrifugation. Surprisingly, all peptides showed an early stage nonfibrillar aggregate or, in the case of Aβ39E22Δ, a fibrillar aggregate that suggests that such extracellular aggregates can be relocated from the outside to the inside of a cell as an aggregate.

MATERIALS AND METHODS

Peptides. Human Aβ1−40, with the sequence DAEFRHDSGYEVHHQKLVFFAEDVGSNKGAIIGLMVGGVV, Aβ1−40H13G with the sequence DAEFRHDSGYEVGHQKLVFFAEDVGSNKGAIIGLMVGGVV, Aβ1−40H14G with the sequence DAEFRHDSGYEVHGQKLVFFAEDVGSNKGAIIGLMVGGVV, Aβ1−40H13,14G with the sequence DAEFRHDSGYEVGGQKLVFFAEDVGSNKGAIIGLMVGGVV, Aβ1−39EΔ22 with the sequence DAEFRHDSGYEVHHQKLVFFADVGSNKGAIIGLMVGGVV, Aβ1−42 with the sequence DAEFRHDSGYEVHHQKLVFFAEDVGSNKGAIIGLMVGGVVIA, Aβ1−42H13G with the sequence DAEFRHDSGYEVGHQKLVFFAEDVGSNKGAIIGLMVGGVVIA, and Aβ1−41EΔ22 with the sequence DAEFRHDSGYEVHHQKLVFFADVGSNKGAIIGLMVGGVVIA were synthesized with or without Ahx (Fmoc-6-aminohexanoic acid) attached to the N-terminus for subsequent coupling with fluorescein as previously described by Poduslo et al.[7] The molecular weight of each peptide was determined by electrospray ionization mass spectrometry (Thermoelectron Surveyor MSQ): 4329 for Aβ1−40, 4801 for F-Aβ1−40, 4200 for Aβ1−39E22Δ, 4671 for F-Aβ1−39E22Δ, 4721 for F-Aβ1−40H13G, 4721 for F-Aβ1−40H14G, 4639 for F-Aβ1−40H13,14G, 4514 for Aβ1−42, 4985 for F-Aβ1−42, 4905 for F-Aβ1−42H13G, and 4385 for Aβ1−41E22Δ.

Cell Culture. PC12 cells were maintained in Dulbecco's modified Eagle's medium (DMEM) (Invitrogen, Carlsbad, CA) supplemented with 10% horse serum (Invitrogen), 10% newborn calf serum (Invitrogen), penicillin (100 units/mL) (Invitrogen), and streptomycin (100 μg/mL) (Invitrogen) in 5% CO_2 at 37 °C. Cells were plated at a density of 2.5−3.0 × 10^4 cells/well in six-well plates (Becton Dickinson, Franklin Lakes, NJ) coated with poly-L-lysine (100 μg/mL) (Sigma, St. Louis, MO) and allowed to differentiate for 6−7 days in medium supplemented with 100 ng/mL nerve growth factor (Harlan Biosciences, Indianapolis, IN). Cells displayed multiple dendritic processes with occasional extended axons.

Membrane Association and Internalization of F-Aβ Peptides. PC12 cells were equilibrated at 37 °C with Hank's Balanced Salt Solution (HBSS) (Mediatech, Inc., Manassas, VA) supplemented with 10 mM Hepes (pH 7.4) (Calbiochem, La Jolla, CA) for 10−30 min prior to the start of the experiment. After equilibration, cells were incubated with either HBSS alone, HBSS containing 10 μg/mL Alexa Fluor 633 transferrin (Invitrogen), or HBSS containing 2.5−10.7 μM F-Aβ peptides for 60 min at 37 °C. Prior to some experiments, concentrated F-Aβ peptides (5 μM) were incubated at 4 °C for 50−60 min. Peptides incubated for 50 min at 4 °C were then incubated for an additional 10 min in the dark at room temperature. All peptides were diluted to their plating concentration of 2.5 μM. Following treatment, cells were removed from each well with either a nonenzymatic cell dissociation solution (Sigma) or 0.0125% trypsin (Invitrogen). Each sample was added to a 12 × 75 polystyrene tube (Becton Dickinson) containing DMEM supplemented with 10% horse serum, 10% newborn bovine serum, penicillin (100 units/mL), and streptomycin (100 μg/mL). Samples were centrifuged at 1000 rpm for 5−8 min. Supernatants were removed and the cells resuspended in Dulbecco's phosphate-buffered saline (DPBS) (Invitrogen) prior to centrifugation. Supernatants were removed and cells fixed in 1% formaldehyde (Ted Pella, Inc., Redding, CA). The cells were analyzed on either a FACSCalibur or a FACSCanto flow cytometer (Becton Dickinson). Fluorescein excitation was at 488 nm, and Alexa Fluor excitation was at 635 nm. Fluorescein emission fluorescence was detected with a 530 ± 15 nm filter, while a 660 ± 10 nm filter was used to detect the emission of Alexa Fluor 633. Forward-angle scatter, side scatter, and geometric mean fluorescent intensities were recorded with 5000−25000 cells and analyzed using CellQuest Pro (Becton Dickinson). Only cells above a forward-angle scatter threshold, distinguishing cells that could be evaluated, were analyzed. Statistical significance between geometric means was determined by one-way analysis of variance (ANOVA) with a Newman−Keuls post

test or a Student's t test using GraphPad Prism 4 (GraphPad Software, La Jolla, CA).

Fluorescence Anisotropy. Aβ40, Aβ39E22Δ, Aβ42, and Aβ41E22Δ peptide solutions were prepared by solubilizing each peptide in DMSO (Sigma) prior to the addition of 0.01 M sodium phosphate (pH 7.4) containing 0.01% (w/v) NaN_3. The final concentration of DMSO was 2% (v/v). Peptide solutions were also prepared without DMSO via addition of 0.01 M sodium phosphate (pH 7.4) containing 0.01% (w/v) NaN_3 directly to each peptide. The final peptide concentration for all experiments was 100 μM.

All anisotropy experiments were conducted using the QuantaMaster 2001-7 T-format steady state spectrofluorometer with temperature control from Photon Technology International, Inc. (London, ON). Samples were excited at 275 nm with the presample polarizer in the vertical position (V, 0°). Emission spectra from 290 to 330 nm were recorded following postsample polarization in the vertical position (V, 0°) and the horizontal position (H, 90°). Next, samples were excited at 275 nm with the presample polarizer in the horizontal position (H, 90°). Emission spectra from 290 to 330 nm were recorded following postsample polarization in the vertical position (V, 0°) and the horizontal position (H, 90°). Spectra were recorded every 100 s for the first 11 min and 40 s and every 10 min from 20 to 60 min. Fluorescence values from 300 to 315 nm were averaged prior to the calculation of anisotropy (A), which was defined as follows:

$$A = I_{VV} - GI_{VH}/I_{VV} + 2GI_{VH}$$

where G corrects for any polarization bias of the detection system.[13] G was defined as follows:

$$G = I_{HV}/I_{HH}$$

Peptides with or without DMSO with or without Centrifugation. Peptide solutions were prepared by adding 0.01 M sodium phosphate (pH 7.4) containing 0.01% (w/v) NaN_3 directly to the peptide. Peptide solutions were also prepared by first solubilizing peptides in DMSO (Sigma) prior to the addition of 0.01 M sodium phosphate (pH 7.4) containing 0.01% (w/v) NaN_3 with the final peptide concentration being 100 μM. For peptide preparations containing DMSO, the final concentration was 2% (v/v). Samples were prepared for TEM. Meanwhile, all remaining sample was spun at a low speed (9600g) for 10 min and allowed to sit while unspun samples were imaged and then spun briefly prior to being spotted on carbon-coated Formvar 300 mesh copper grids (Electron Microscopy Sciences, Hatfield, PA) prior to imaging.

HFIP Treatment of Peptides. Peptides were placed in nonsiliconized tubes and solubilized in cold 1,1,1,3,3,3-hexafluoro-2-propanol (HFIP) at a concentration of 1 μg/μL. Peptides were allowed to stand at room temperature for 50 min prior to being placed on ice for 10 min. Samples were aliquoted, 100 μg per vial, into 2.0 mL screwtop vials (Nalgene-Nunc, Rochester, NY) and allowed to dry uncovered overnight. The next morning, samples were dried for 10 min using a SpeedVac Concentrator (ThermoScientific, Waltham, MA) prior to being stored desiccated at −20 °C. Before being used, peptides were warmed to room temperature and solubilized in DMSO prior to the addition of 0.01 M sodium phosphate (pH 7.4) containing 0.01% (w/v) NaN_3. The final concentration of DMSO was 2% (v/v), and the final peptide concentration was 100 μM.

Transmission Electron Microscopy. Peptides were solubilized in 0.01 M sodium phosphate (pH 7.4) containing 0.01% (w/v) NaN_3 alone or dissolved in DMSO prior to being diluted with sodium phosphate. The final peptide concentration was 100 μM, and in the studies involving DMSO, the final DMSO concentration was 2% (v/v). Carbon-coated Formvar 300 mesh copper grids (Electron Microscopy Sciences) were spotted with 3 μL of the peptide sample and allowed to stand for 1 min. The solution was wicked away with filter paper, and the peptide was rinsed twice with 3 μL of nanopure water. The negative stain was performed using 3 μL of 0.1% uranyl acetate and the sample allowed to sit briefly prior to removal. Each grid was rinsed twice more with 3 μL of nanopure water and allowed to dry. The entire staining process took 5−10 min depending on the number of grids stained. Grids were air-dried and imaged. Micrographs were imaged on a JEOL 1400 TEM microscope (JEOL Ltd., Tokyo, Japan) at magnifications of 15000×, 60000×, and 100000×. For time course studies, peptides were incubated in a 96-well black microplate (Greiner), covered with sealing film and a black lid, and placed on an Innova40 incubator shaker (New Brunswick Scientific, Edison, NJ) for 0, 1, 2, 4, 8, and 24 h at 37 °C at 300 rpm. Aliquots were taken at each time point and prepared for TEM analysis.

Atomic Force Microscopy. Aβ39E22Δ and F-Aβ39E22Δ peptides were solubilized in 0.01 M sodium phosphate (pH 7.4) containing 0.01% (w/v) NaN_3 to a concentration of 100 μM. Peptides were added to a 96-well black microplate (Greiner) in which an aliquot of each peptide was removed and diluted to a final concentration of 1 μM in 0.01 M sodium phosphate (pH 7.4) containing 0.01% (w/v) NaN_3. Immediately, 10 μL of sample was added to a freshly cleaved layer of mica (Ted Pella, Inc.) and allowed to air-dry. The remaining peptides were incubated for 1 h at 37 °C using an Innova 40 incubator shaker (New Brunswick). Following incubation, peptides were diluted to 1 μM in 0.01 M sodium phosphate (pH 7.4). Ten microliters of the sample was added to freshly cleaved mica and allowed to air-dry. Atomic force microscopy (AFM) measurements were taken on dry peptide samples with silicon nitride NP-S20 tips (Veeco Metrology, Inc., Santa Barbara, CA) using a MultiMode Scanning Probe Microscope (MM SPM) with a NanoScope IV controller. A high-resolution J-type scanner was used to scan the peptide surface. Images were collected by raster scanning across a 10 μm^2 area at 1024 samples (pixels) per line at a rate of 3.70 Hz. Images were processed with NanoScope software (Veeco Metrology, Inc.).

Fibril Formation. Peptides were solubilized in 0.01 M sodium phosphate (pH 7.4) containing 0.01% (w/v) NaN_3 so that the final concentration was 100 μM. Peptides were incubated as described above for 7 days. Like peptide samples from the 96-well plate were pooled in a 12 mm × 75 mm borosilicate glass tube (Fisher Scientific). For each pooled peptide sample, a 2.5 μM plating solution was prepared in HBSS (Mediatech, Inc.) supplemented with 10 mM Hepes (pH 7.4) (Calbiochem), with the remaining pooled samples being sonicated for 5 min prior to being diluted to 2.5 μM in HBSS/Hepes buffer. Fibrils with or without sonication were then used in F-Aβ peptide binding studies as described above.

Internalization of F-Aβ Peptides and Their Fibrils. F-Aβ40 and F-Aβ39E22Δ fibrils were prepared as previously described. Following the 7 day incubation, 2.5 μM peptide and fibril (with or without sonication) solutions were prepared in HBSS (Mediatech, Inc.) supplemented with 10 mM Hepes

(pH 7.4) (Calbiochem) and used in F-Aβ peptide internalization studies as described above, where differentiated PC12 cells were incubated with HBSS/Hepes buffer alone, fluorescein-labeled Aβ peptide fibrils with or without sonication (2.5 μM), or transferrin conjugated to Alexa Fluor 633 (10 μg/mL) at 37 °C for 1 h. Following incubation, two wells each of F-Aβ40 and F-Aβ39E22Δ sonicated fibrils were acid stripped with HBSS/Hepes buffer (pH 3.5) for 10 s. All cells were harvested using trypsin as previously described. Cellular fluorescence was obtained from flow cytometry analysis. The geometric mean fluorescence intensity (n = 3) was determined using CellQuest Pro.

Accumulation of F-Aβ40 and F-Aβ39E22Δ Peptides and Fibrils in the Acidic Compartment. After being preincubated in Hank's Balanced Salt Solution containing 10 mM Hepes buffer (HBSS/Hepes) for 15 min at 37 °C, the differentiated PC12 cells grown on coverslip bottom dishes (MatTek, Ashland, MA) were incubated in HBSS/Hepes buffer containing 2.5 μM F-Aβ40, F-Aβ40 fibrils (sonicated or unsonicated), F-Aβ39E22Δ, or F-Aβ39E22Δ fibrils (sonicated or unsonicated) at 37 °C. After incubation for 40 min, 75 nM Lysotracker Red (Invitrogen-Molecular Probes, Carlsbad, CA) was added to the dishes, and the dishes were allowed to incubate for an additional 20 min. Thereafter, the cells were washed three times with PBS and imaged using Axiovert 100M microscope equipped with an LSM 510 system (Carl Zeiss MicroImaging, Inc., Thornwood, NY). F-Aβ was imaged with a 200 mW argon ion laser ($\lambda_{excitation}$ = 488 nm, and $\lambda_{excitation}$ = 505 nm), whereas the Lysotracker Red (LR) was visualized with a 543 nm line of a HeNe laser and a 560−615 nm BP filter.

RESULTS

Binding of F-Aβ Mutations and Deletions to PC12 Neurons. The neuronal cell culture model of pheochromocytoma (PC12) differentiated with nerve growth factor-containing medium was used to assess the binding of fluorescein-labeled Aβ40 (F-Aβ40), F-Aβ40H13G, F-AβH14G, and F-AβH13,14G by flow cytometry analysis. Shifts in the histograms of cellular fluorescence indicated mostly membrane-associated and/or cellular uptake of F-Aβ40 with differentiated PC12 cells (Figure 1). In addition to the cells being incubated with F-Aβ, transferrin conjugated to Alexa Fluor 633 was also included as a marker of endocytosis and healthy, viable cells. Comparison of the geometric mean fluorescence intensity of neurons treated with F-AβH13,14G demonstrated weaker binding compared to neurons that were treated with F-Aβ40, thus confirming our previous observation.[7] Cells that were treated with nonenzymatic cell dissociation medium displayed cellular fluorescence from both internalized and membrane-associated peptide (Figure 1A). In contrast, treatment of cells with trypsin removes the membrane-associated peptide and represents fluorescence-internalized protein only (Figure 1B). The geometric mean fluorescence intensity of neurons treated with trypsin was lower than those treated with cell dissociation buffer. Transferrin levels were similar between neurons treated with trypsin and cell dissociation buffer. Therefore, trypsin digestion reflects neuronal internalization that occurs during the 1 h incubation. Substitution of histidine with glycine decreased the level of neuronal binding and internalization in the following order: H13G < H14G < H13,14G. A dose-dependent increase in the geometric mean fluorescence intensity was seen with increasing concentrations of F-Aβ39E22Δ (Figure 2). At the same dose

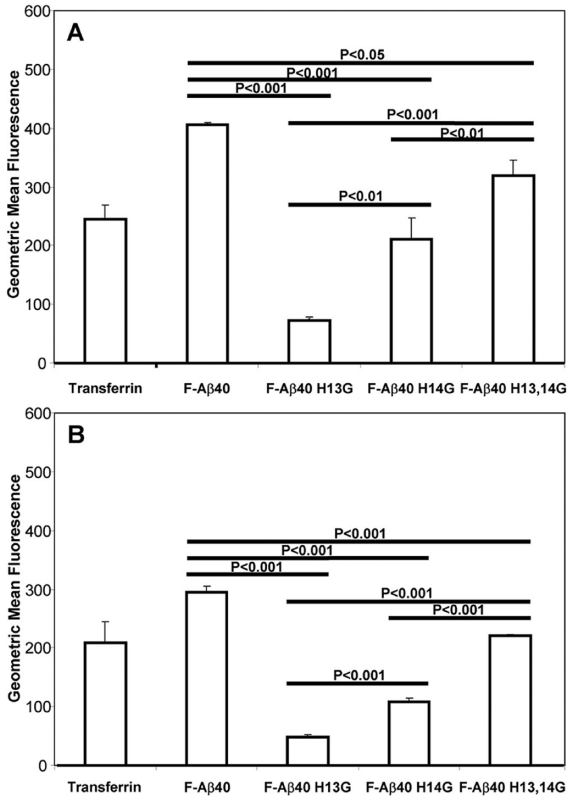

Figure 1. Weakened neuronal binding of Aβ40 in the following order: H13G < H14G < H13,14G. PC12 cells were incubated with fluorescein-labeled Aβ peptides (2.5 μM) or transferrin conjugated to Alexa Fluor 633 (10 μg/mL) at 37 °C for 1 h. Prior to incubation with cells, concentrated fluorescein-labeled Aβ peptides (5.0 μM) were incubated at 4 °C for 50 min followed by a 10 min incubation at room temperature. Fluorescein-labeled Aβ peptides were diluted to a plating concentration of 2.5 μM with Hank's Balanced Salt Solution containing 10 mM Hepes (pH 7.4). Following incubation, cells were harvested using either nonenzymatic cell dissociation medium (A) or trypsin (B). Cellular fluorescence was obtained from flow cytometry analysis. The geometric mean fluorescence intensities (n = 3) were determined using CellQuest Pro and were significantly different as determined by one-way ANOVA. Following the one-way ANOVA, a Newman−Keuls multiple-comparison test was performed.

(25 μg/mL), F-Aβ39E22Δ showed a 6-fold increase in its level of binding compared to that of F-Aβ40, indicating that the level of neuronal internalization of Aβ is increased by deletion of glutamate 22 in a dose-dependent manner. As shown in Figure 3, the H13G substitution of F-Aβ39E22Δ does not weaken neuronal binding for F-Aβ40. Also shown in Figure 3 is a separate experiment comparing F-Aβ42 and F-Aβ42H13G that showed that the H13G substitution had no effect on neuronal uptake. From these studies, the mechanism of neuronal binding/internalization of Aβ40 is hypothesized to be different from that of Aβ39E22Δ and Aβ42 and possibly related to the rapidity of aggregation of Aβ39E22Δ. To further assess the aggregation of Aβ39E22Δ compared to that of the other peptides, fluorescence anisotropy studies were performed.

Fluorescence Anisotropy of Aβ40 and Aβ42 with or without DMSO Treatment. Fluorescence anisotropy experiments were performed to evaluate the early stages of aggregation of Aβ40 and Aβ42 with and without DMSO by following tyrosine at position 10. Measurements of all peptides were taken at 100 μM. Figure 4A shows the fluorescence

dx.doi.org/10.1021/bi300275g | Biochemistry 2012, 51, 3993−4003

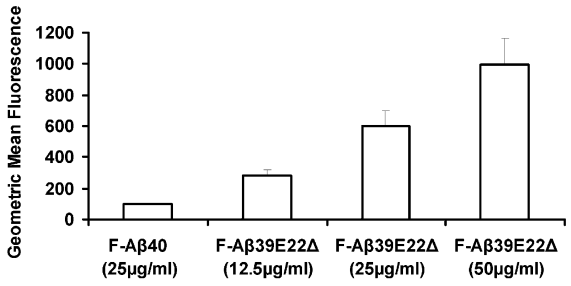

Figure 2. F-Aβ39E22Δ dose−response neuronal binding. PC12 cells were incubated with increasing doses of fluorescein-labeled Aβ39E22Δ peptide (12.5, 25, and 50 μg/mL, which equal 2.7, 5.4, and 10.7 μM, respectively) or 25 μg/mL (5.2 μM) fluorescein-labeled Aβ40 for 1 h at 37 °C and were harvested using trypsin. Cellular fluorescence was obtained from flow cytometry analysis. The geometric mean fluorescence intensity (n = 3) was determined using CellQuest Pro. Geometric means were normalized prior to statistical analysis using a one-way ANOVA with a Newman−Keuls multiple-comparison test. Our data showed the F-Aβ39E22Δ peptide behaves in a dose-dependent manner with the concentrations of 25 and 50 μg/mL being significantly different (p < 0.001) from that of F-Aβ40 (25 μg/mL).

anisotropy of Aβ40 with and without DMSO treatment. As one can see, there was no difference caused by the treatment with DMSO, and the anisotropy value was substantially low at all times through 60 min. This anisotropy of Aβ40 remained

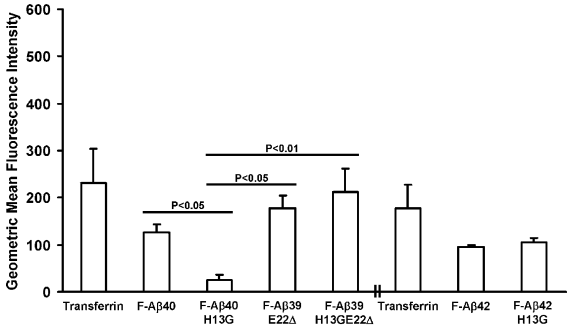

Figure 3. Enhanced neuronal uptake is observed with F-Aβ39E22Δ, while F-Aβ40 in the prescence of the H13G mutation shows weakened neuronal uptake. The H13G mutation in conjunction with F-Aβ39E22Δ and F-Aβ42 has no significant effect on uptake. PC12 cells were incubated with fluorescein-labeled Aβ peptides (2.5 μM) or transferrin conjugated to Alexa Fluor 633 (10 μg/mL) at 37 °C for 1 h. Prior to incubation with cells, concentrated (5.0 μM) fluorescein-labeled Aβ peptides (F-Aβ40, F-Aβ40H13G, F-Aβ39E22Δ, and F-Aβ39E22ΔH13G) were incubated at 4 °C for 1 h. These peptides were diluted to a concentration of 2.5 μM with Hank's Balanced Salt Solution containing 10 mM Hepes (pH 7.4) before being added to cells. Following incubation, cells were harvested using trypsin. Cellular fluorescence was obtained from flow cytometry analysis. The geometric mean fluorescence intensity (n = 3) was determined using CellQuest Pro. Either a one-way ANOVA with a Newman−Keuls multiple-comparison test (F-Aβ40, F-Aβ40H13G, F-Aβ39E22Δ, and F-Aβ39E22ΔH13G) or a Student's t test (F-Aβ42 and F-Aβ42H13G) was performed to determine significance. Our data show the F-Aβ40H13G geometric mean is significantly lower than that of F-Aβ40 (p < 0.05) while the geometric mean of F-Aβ39E22ΔH13G is not significantly different from that of F-Aβ39E22Δ (p > 0.05), indicating that the H13G mutation on F-Aβ39E22Δ did not decrease the level of internalization by PC12 cells as it does for F-Aβ40. The H13G mutation on F-Aβ42 also did not decrease the level of internalization by PC12 cells.

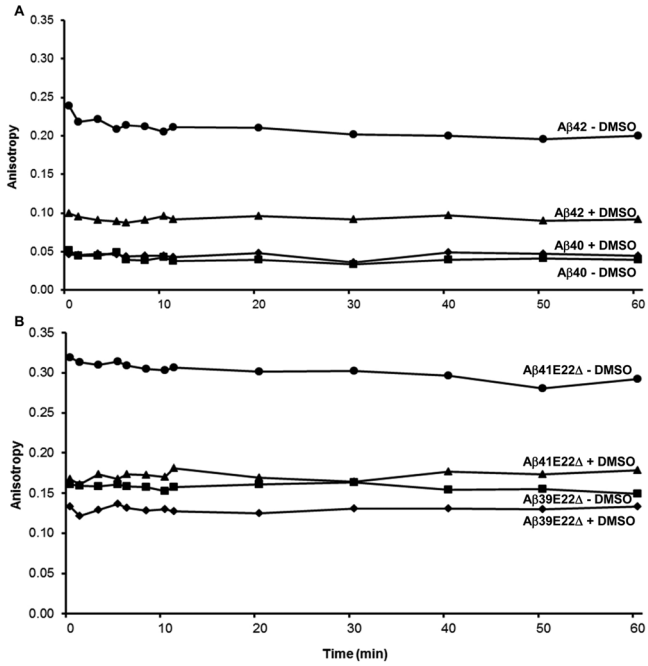

Figure 4. (A) Fluorescence anisotropy of Aβ40 (■) and Aβ40 (◆) with DMSO treatment and Aβ42 (●) and Aβ42 (▲) without DMSO treatment. Peptide solutions (100 μM) were prepared by directly solubilizing the peptide in 0.01 M sodium phosphate (pH 7.4) containing 0.01% (w/v) NaN_3 or by first solubilizing the peptide in DMSO prior to the addition of 0.01 M sodium phosphate (pH 7.4) containing 0.01% (w/v) NaN_3 with a final DMSO concentration of 2% (v/v). Anisotropy was calculated as described in Materials and Methods from polarized fluorescence measurements conducted over 1 h. Anisotropy means were averaged from three independent experiments and graphed vs time. (B) Fluorescence anisotropy of Aβ39E22Δ (■) and Aβ39E22Δ (◆) with DMSO treatment and Aβ41E22Δ (●) and Aβ41E22Δ (▲) without DMSO treatment. Peptide solutions (100 μM) were prepared as described in Materials and Methods. Fluorescence anisotropy measurements were conducted over 1 h and used to calculate anisotropy as described in Materials and Methods. Anisotropy means, for each peptide, were averaged from three independent experiments and graphed vs time.

constant over the course of the experiment, indicating that no change in rigidity occurs for tyrosine. In contrast, Aβ42 without DMSO treatment resulted in a significantly higher anisotropy, indicating increased rigidity of the tyrosine residue within the Aβ42 peptide (Figure 4A). Treatment of Aβ42 with DMSO resulted in a decrease in the anisotropy to a level of 0.10, which was substantially higher than that of Aβ40, indicating that DMSO has the ability to decrease the tyrosine rigidity in Aβ42.

Fluorescence Anisotropy of Aβ39E22Δ and Aβ41E22Δ with or without DMSO Treatment. The fluorescence anisotropy of Aβ39E22Δ without DMSO treatment was constant over the time range studied with a value of approximately 0.15 (Figure 4B). This value was substantially higher than that of Aβ40 and higher than that of Aβ42 with DMSO treatment (as observed in Figure 4A). DMSO treatment showed had an only modest effect on Aβ39E22Δ. In contrast, Aβ41E22Δ without DMSO treatment showed an anisotropy of 0.30, which indicated nearly complete rigidity of the tyrosine residue within the peptide.[13] Treatment with DMSO decreased the anisotropy level to ~0.17, which was higher than that of AβE39E22Δ either with or without DMSO pretreatment. It is clear that DMSO treatment decreases the

dx.doi.org/10.1021/bi300275g | Biochemistry 2012, 51, 3993−4003

rigidity of Aβ41E22Δ and Aβ42 to a significant extent, but this rigidity was still substantially greater than that of Aβ40. These experiments demonstrate that Aβ39E22Δ, Aβ41E22Δ, and Aβ42 have increased tyrosine rigidity compared to that of Aβ40, suggesting that these peptides may be aggregating into comparable amyloid structures. This was further evaluated by sampling aliquots of the peptides at various times for examination by electron microscopy.

Transmission Electron Microscopy of Aβ39E22Δ and Aβ41E22Δ. The peptides were solublized in 0.01 M sodium phosphate (pH 7.4) containing 0.01% (w/v) NaN_3 with a final peptide concentration of 100 μM. As indicated in Materials and Methods, the peptides were spotted on carbon-coated Formvar copper grids. The solution was wicked away, rinsed twice with water, negatively stained with 0.1% uranyl acetate, rinsed several times with water, and allowed to dry. The entire process from initial solubilization to spotting for TEM took <10 min (baseline). Figure 5 shows the TEM of Aβ39E22Δ at baseline

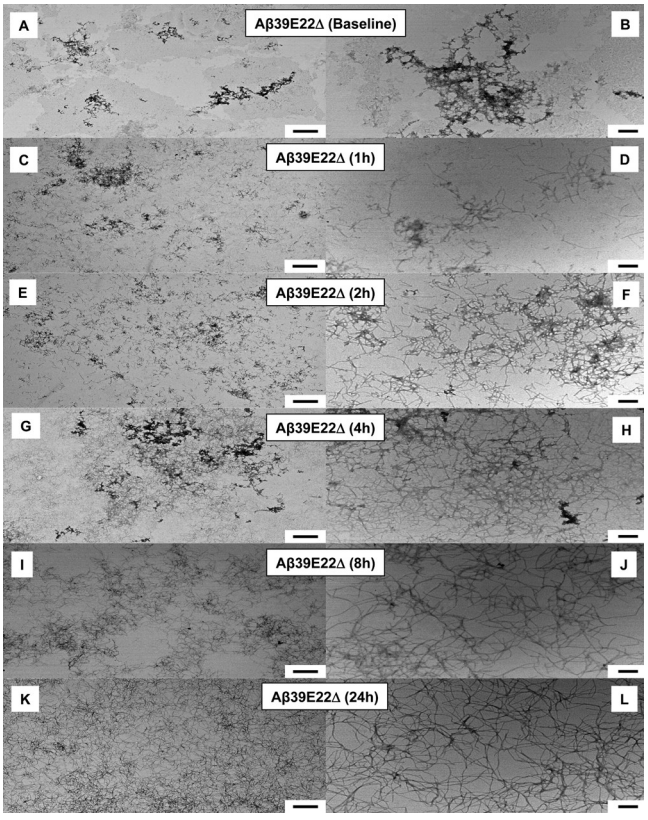

Figure 5. TEM of Aβ39E22Δ. The Aβ39E22Δ peptide (100 μM) prepared in sodium phosphate buffer was incubated at 37 °C while being shaken for a period of 24 h. Samples were obtained for TEM at baseline (<10 min) and at 1, 2, 4, 8, and 24 h as described in Materials and Methods. Panels A, C, E, G, I, and K are images taken at 15000× magnification (scale bar of 1 μm), while panels B, D, F, H, J, and L are images taken at 60000× magnification (scale bar of 200 nm).

with samples and subsequent images taken at 1, 2, 4, 8, and 24 h. As one can see at baseline, Aβ39E22Δ showed aggregate formation with some suggestion of fibrils. Fibrils became more apparent at 1 h and progressively increased in number over the time course. In contrast, Aβ41E22Δ showed similar aggregates at baseline through 4 h, with beginning fibril formation at 8 and 24 h (Figure 6). Aβ41E22Δ clearly showed delayed fibril formation as compared to fibrils that were rapidly formed with

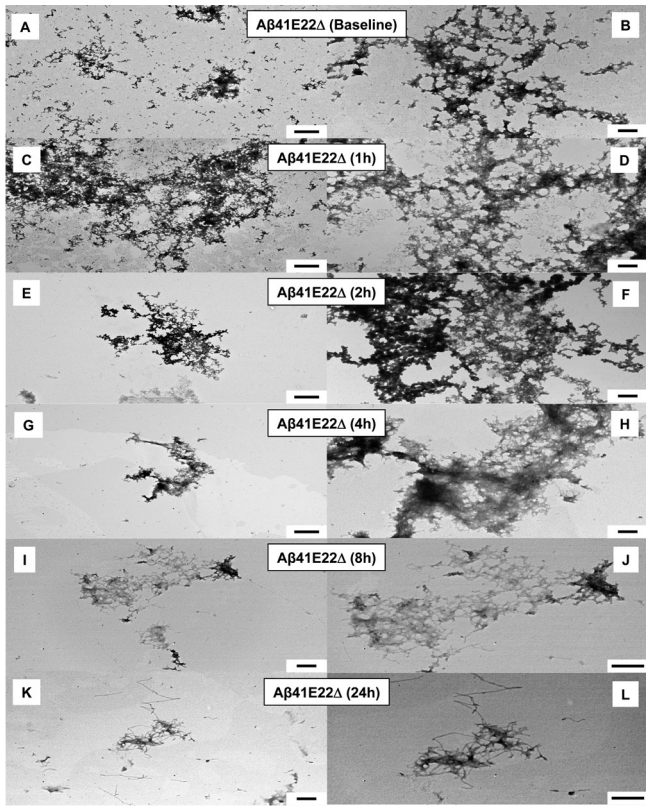

Figure 6. TEM of Aβ41E22Δ. The Aβ41E22Δ peptide (100 μM) prepared in sodium phosphate buffer was incubated at 37 °C while being shaken for a period of 24 h. Samples were obtained for TEM at baseline (<10 min) and at 1, 2, 4, 8, and 24 h as described in Materials and Methods. Panels A, C, E, and G are images taken at 15000× magnification (scale bar of 1 μm), while panels B, D, F, H, I, and K are images taken at 60000× magnification (scale bar of 200 nm). Panels J and L are images taken at 100000× magnification (scale bar of 200 nm).

Aβ39E22Δ. This is possibly related to the intense tyrosine rigidity observed with Aβ41E22Δ at 1 h (Figure 4B).

Time Course TEM of Aβ40 and Aβ42. Figures 7 and 8 show the TEM of Aβ40 and Aβ42, respectively, at baseline with samples and subsequent images taken at 1, 2, 4, 8, and 24 h. Aβ40 showed aggregates through all the time points except 24 h, where fibrils were observed. In contrast, aggregates predominated for Aβ42 through only 4 h with the first appearance of fibrils at 8 h. It is clear that the predominant species at baseline for all peptides is an early stage nonfibrillar aggregate with only Aβ39E22Δ having fibrils at 1 h.

TEM of Aβ40 and Aβ42 with or without DMSO or HFIP Treatment or Centrifugation. Because organic solvents are often used to defibrillize Aβ proteins, we next evaluated Aβ40 and Aβ42 before and after treatment with DMSO or after centrifugation at a low speed (9600g). As shown in Figure 9, no changes were observed in the aggregates formed following DMSO treatment or centrifugation. Figure 10 also shows no effects of HFIP on the aggregates formed for both Aβ40 and Aβ42.

TEM of F-Aβ40 and F-Aβ39E22Δ. To verify that fluorescein modification of Aβ at the N-terminal ASP residue did not affect subsequent aggregate or fibril formation, TEM analysis was done on F-Aβ40 and F-Aβ39E22Δ (Figure 11). F-Aβ40 at baseline showed aggregate formation similar to that of

dx.doi.org/10.1021/bi300275g | *Biochemistry* 2012, 51, 3993−4003

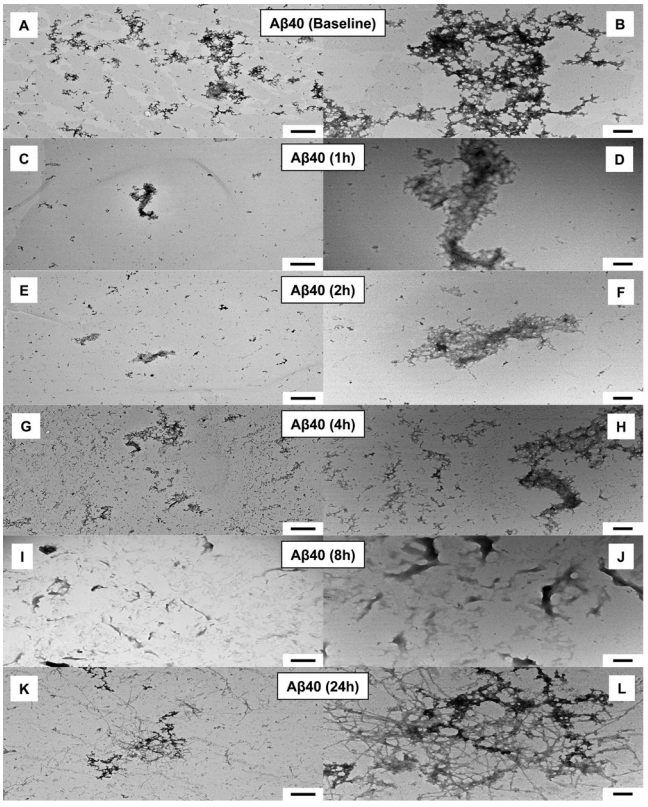

Figure 7. TEM of Aβ40. The Aβ40 peptide (100 μM) prepared in sodium phosphate buffer was incubated at 37 °C while being shaken for a period of 24 h. Samples were obtained for TEM at baseline (<10 min) and at 1, 2, 4, 8, and 24 h as described in Materials and Methods. Panels A, C, E, G, I, and K are images taken at 15000× magnification (scale bar of 1 μm), while panels B, D, F, H, J, and L are images taken at 60000× magnification (scale bar of 200 nm).

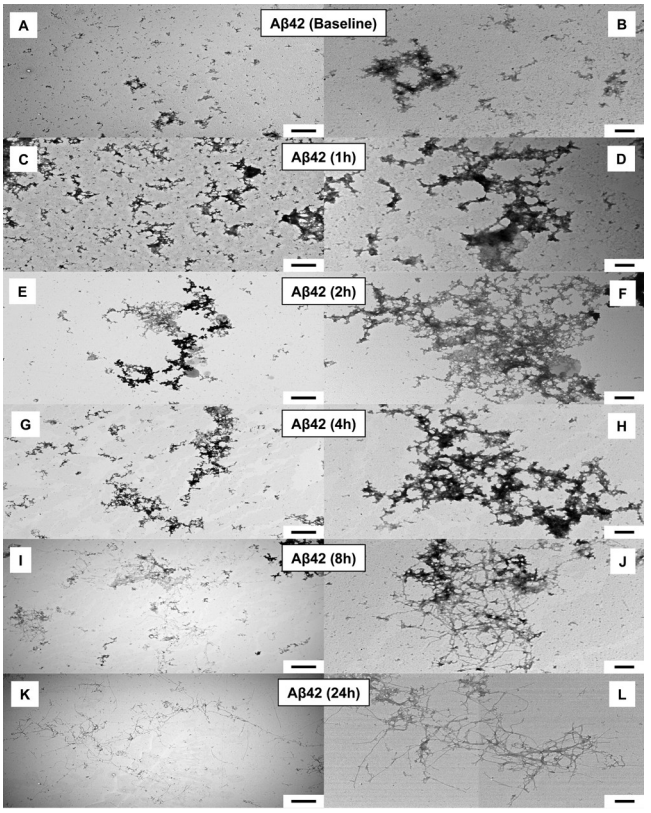

Figure 8. TEM of Aβ42. The Aβ42 peptide (100 μM) prepared in sodium phosphate buffer was incubated at 37 °C while being shaken for a period of 24 h. Samples were obtained for TEM at baseline (<10 min) and at 1, 2, 4, 8, and 24 h as described in Materials and Methods. Panels A, C, E, G, I, and K are images taken at 15000× magnification (scale bar of 1 μm), while panels B, D, F, H, J, and L are images taken at 60000× magnification (scale bar of 200 nm).

Aβ40 (see Figure 7). In contrast, F-Aβ39E22Δ showed a higher level of fibril formation compared to that of Aβ39E22Δ at baseline (see Figure 5). These experiments confirm that modification of the N-terminal aspartic acid (Asp) residue with fluorescein does not restrict subsequent aggregate or fibril formation.

AFM of Aβ39E22Δ at Baseline and 1 h with or without Fluorescein. Panels A and B of Figure 12 demonstrate by AFM aggregates of Aβ39E22Δ at baseline with early stage fibrils and extensive fibrils at 1 h, thus confirming the TEM observations (Figure 5). F-Aβ39E22Δ had more fibrils at baseline and substantially large fibrils at 1 h. Similar results were observed by TEM (Figure 9); thus, N-terminal modification of Aβ with fluorescein did not affect the ability of the peptide to form aggregates or fibrils.

TEM of F-Aβ40 Fibrils and F-Aβ39E22Δ Fibrils with or without Sonication and Their Internalization to PC12 Neurons. Because F-Aβ39E22Δ exhibited extensive fibrils at baseline (Figure 11) with an increased level of internalization to PC12 neurons (Figure 2), we evaluated fibrils that were formed after 7 days. As shown in Figure 13, fibrils of F-Aβ39E22Δ with or without sonication (Figure 13C,D) showed internalization comparable to that of F-Aβ39E22Δ that was incubated with the neurons for only 1 h (Figure 13E). Sonicated F-Aβ39E22Δ fibrils that were incubated with neurons followed by an acid strip prior to trypsin removal also showed comparable internalization; hence, well-established fibrils of F-Aβ39E22Δ were internalized as efficiently as fibrils formed after incubation for only 1 h. In contrast, F-Aβ40 fibrils with or without sonication (Figure 13A,B) or acid strip showed weakened binding to PC12 cells (Figure 13E), which suggests that H-13 of Aβ40 is masked by the formation of fibrils.

Accumulation of F-Aβ40 and F-Aβ39E22Δ Peptides and Fibrils in the Acidic Compartment. When incubated with F-Aβ40 peptide, differentiated PC12 cells demonstrated partial colocalization with Lysotracker Red that predominantly labels lysosomes (Figure 14A). While the F-Aβ39E22Δ peptide bound to the cell membrane to a much greater extent than the F-Aβ40 peptide, the internalized F-Aβ39E22Δ accumulated almost entirely in the lysosomes indicated by the punctate yellow regions formed from the overlapping green, due to F-Aβ39E22Δ, and red signals, due to Lysotracker Red (Figure 14A′). F-Aβ40 fibrils demonstrated a significantly greater level of accumulation in the lysosomes (Figure 14B). F-Aβ39E22Δ fibrils on the other hand showed similar levels of accumulation in the lysosomes as the peptide, but their level of binding to the cell membranes increased noticeably (Figure 14B′). Whereas the sonicated F-Aβ40 fibrils did not show any changes in their lysosomal accumulation patterns (Figure 14C), sonicated F-Aβ39E22Δ showed enhanced binding to cell membranes compared to the unsonicated fibrils (Figure 14B′,C′).

dx.doi.org/10.1021/bi300275g | *Biochemistry* 2012, 51, 3993−4003

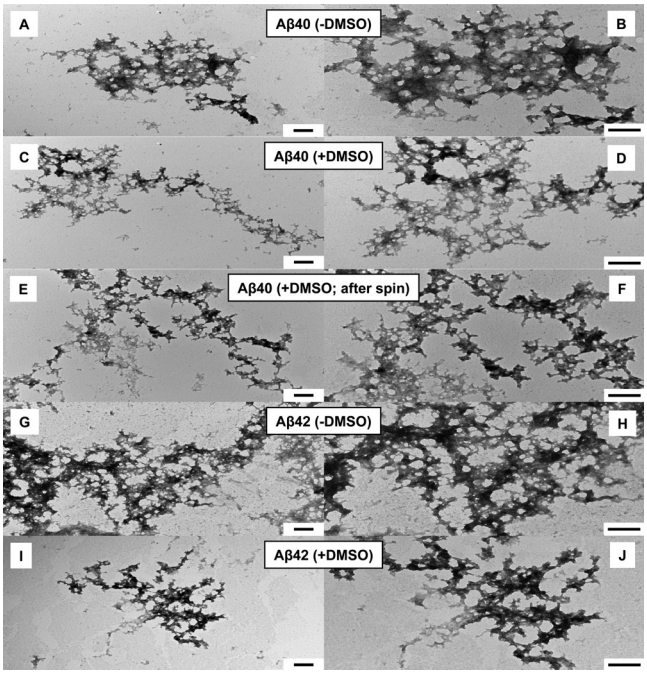

Figure 9. TEM of Aβ peptides before and after DMSO treatment or centrifugation. Peptide solutions (100 μM) were prepared by directly solubilizing the peptide in sodium phosphate buffer or by first solubilizing the peptide in DMSO prior to the addition sodium phosphate buffer as described in Materials and Methods. Initial samples were obtained for TEM immediately following preparation. Aβ40 containing DMSO was further treated by centrifugation of the initial sample at 9600*g* for 10 min. TEM of Aβ40 (100 μM) (A and B) and after DMSO treatment (C and D) or after centrifugation (9600*g*) (E and F). TEM of Aβ42 (100 μM) (G and H) and after DMSO treatment (I and J). Panels A, C, E, G, and I are images taken at 60000× magnification (scale bar of 200 nm), while panels B, D, F, H, and J are images taken at 100000× magnification (scale bar of 200 nm).

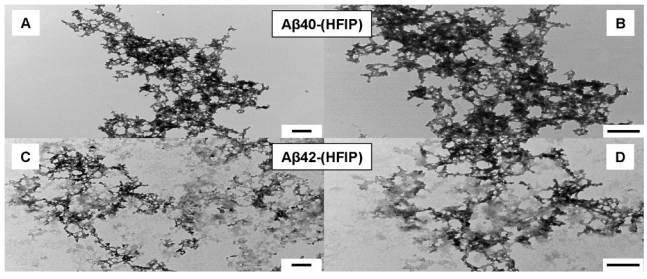

Figure 10. TEM of Aβ40 and Aβ42 peptides treated with HFIP. Aβ40 and Aβ42 peptides were solubilized in 1,1,1,3,3,3-hexafluoro-2-propanol (HFIP) and allowed to dry. Peptide solutions (100 μM) were prepared by solubilizing each peptide in DMSO prior to the addition of sodium phosphate buffer. TEM of Aβ40 (100 μM) after HFIP treatment (A and B) and Aβ42 (100 μM) after HFIP treatment (C and D). Panels A, and C are images taken at 60000× magnification (scale bar of 200 nm), while panels B, and D are images taken at 100000× magnification (scale bar of 200 nm).

DISCUSSION

The pathogenesis of AD clearly involves neuronal degeneration, which is likely manifested by the intraneuronal accumulation of Aβ. Defining the structural basis of neuronal binding and accumulation might provide novel therapeutic targets for blocking this early event associated with the eventual neuronal

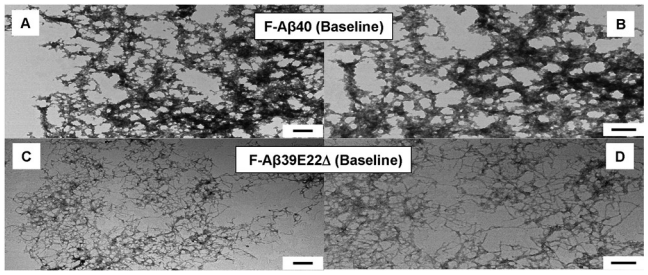

Figure 11. TEM of F-Aβ40 and F-Aβ39E22Δ. Peptide solutions (100 μM) were prepared by directly solubilizing the peptide in sodium phosphate buffer as described in Materials and Methods. Samples were obtained for TEM at baseline (<10 min) and prepared for imaging as described in Materials and Methods. F-Aβ40 (100 μM) at baseline (A and B) and F-Aβ39E22Δ (100 μM) at baseline (C and D). Panels A, and C are images taken at 60000× magnification (scale bar of 200 nm), while panels B, and D are images taken at 100000× magnification (scale bar of 200 nm).

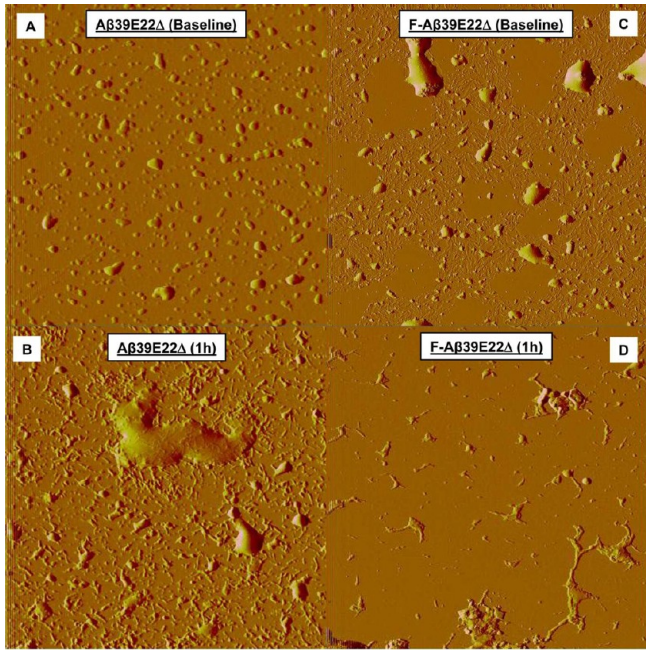

Figure 12. Atomic force microscopy. Aβ39E22Δ and F-Aβ39E22Δ peptides (100 μM) were prepared in sodium phosphate buffer and incubated at 37 °C while being shaken for a period of 1 h. Samples were obtained for AFM at baseline (<10 min) and 1 h. Prior to the peptides being spotted for AFM, they were diluted to 1 μM using sodium phosphate buffer as described in Materials and Methods. AFM of Aβ39E22Δ at baseline (A) and at 1 h (B) and F-Aβ39E22Δ at baseline (C) and at 1 h (D). Deflection images were collected by raster scanning across a 10 μm^2 area at 1024 samples (pixels) per line at a rate of 3.70 Hz.

demise. In this study, we demonstrate that the primary domain on Aβ40 for neuronal binding involves the histidine residue at position 13. Because this substitution does not completely block Aβ40 binding (Figure 1), other yet-to-be-determined regions on Aβ40 may play complementary roles in the binding mechanism.

The extensive intraneuronal accumulation of the variant Aβ lacking glutamate 22 shown in cells transfected with this deletion[9] and in transgenic mice with this deletion[10] provided the opportunity to test whether this deletion strengthened binding in our PC12 assay. A significantly enhanced internal-

dx.doi.org/10.1021/bi300275g | *Biochemistry* 2012, 51, 3993−4003

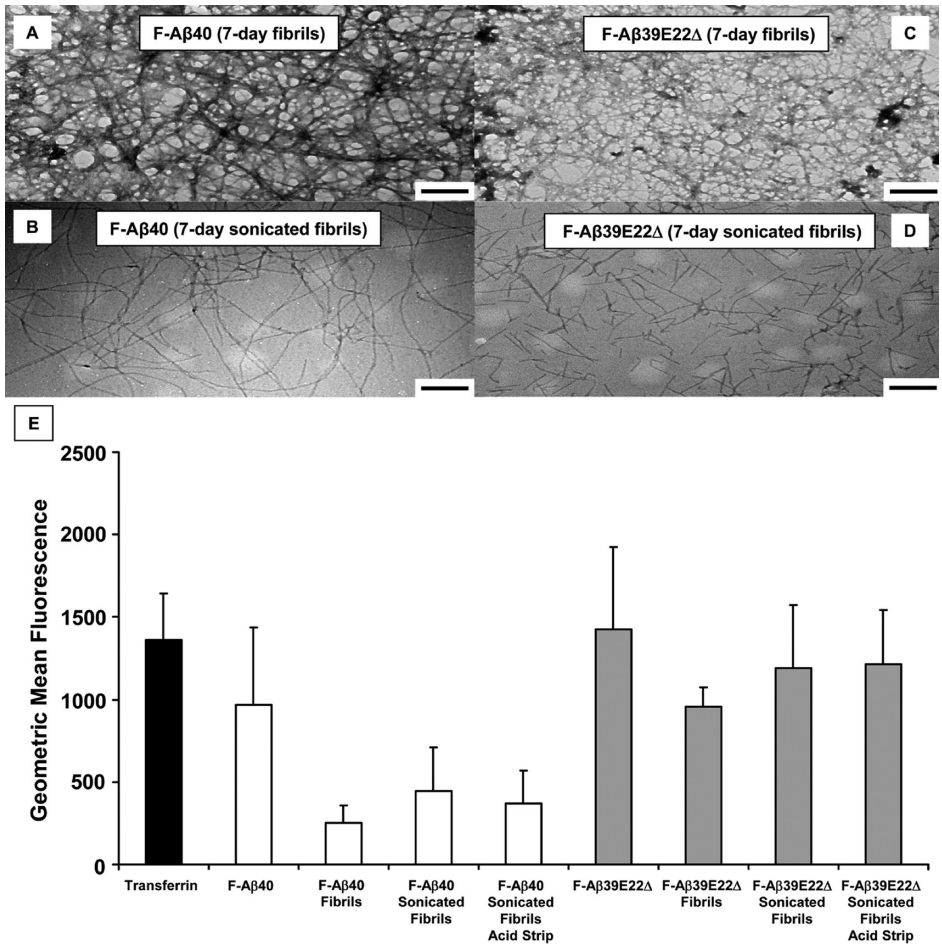

Figure 13. F-Aβ fibrils binding to PC-12 neurons. F-Aβ40 and F-Aβ39E22Δ fibrils were prepared by solubilizing peptides in 0.01 M sodium phosphate (pH 7.4) containing 0.01% (w/v) NaN_3 so that the final concentration was 100 μM. Peptides were incubated at 37 °C, while being shaken at 300 rpm, for 7 days. Like fibril samples were pooled and used to prepare a 2.5 μM fibril plating solution in HBSS (Mediatech, Inc.) supplemented with 10 mM Hepes (pH 7.4) (Calbiochem). Some fibril samples were also sonicated for 5 min prior to creation of a 2.5 μM sonicated fibril solution in HBSS/Hepes buffer. PC12 cells were incubated with fluorescein-labeled Aβ peptide (2.5 μM) or transferrin conjugated to Alexa Fluor 633 (10 μg/mL) or fibrils at 37 °C for 1 h. Following incubation, two wells each of F-Aβ40 and F-Aβ39E22Δ sonicated fibrils were acid stripped with HBSS/Hepes buffer (pH 3.5) for 10 s. All cells were harvested using trypsin. Cellular fluorescence was obtained via flow cytometry analysis. Panels A–D are TEM images taken at 100000× magnification (scale bar of 200 nm). The geometric mean fluorescence intensity (n = 3) was determined using CellQuest Pro (E).

ization was observed (Figures 2 and 3), which explains the high level of intraneuronal Aβ seen in the transgenic mice. Surprisingly, the H13G mutation in Aβ40E22Δ did not weaken the internalization as it does for Aβ40 (Figure 3). This mutation also did not affect the internalization of Aβ42.

Because of the increased rigidity of the tyrosine at position 10 for the Aβ deletion observed by Cloe et al.,[12] we hypothesized that the H13G substitution on Aβ39E22Δ might be affected by this increased rigidity. Aβ39E22Δ had an anisotropy that was 3 times greater than that of Aβ40 (compare panels A and B of Figure 4) with only modest effects with DMSO treatment. Also, Aβ42 had an anisotropy that was 4 times greater than that of Aβ40. These experiments suggest that the increased tyrosine rigidity of Aβ39E22Δ and Aβ42 likely masks the H13G substitution or that the H13 residue is not required for neuronal binding as it is for Aβ40. Surprisingly, Aβ41E22Δ showed the highest anisotropy followed by Aβ42, both of which were decreased by DMSO treatment (Figures 4). Such increased tyrosine rigidity suggests common aggregate formation with possible early stage fibril formation particularly for Aβ39E22Δ.[12] Aggregate formation was next evaluated by TEM after various periods of incubation.

In support of the TEM studies of Cloe et al.,[12] we observed fibril formation with Aβ39E22Δ at 1 h, the level of which progressively increased over the time course (Figure 5). At baseline (<10 min), Aβ39E22Δ displayed aggregates with evidence of fibrils. In contrast, Aβ41E22Δ showed delayed fibril formation that began at 8 h with prior aggregate formation (Figure 6). Surprisingly, Aβ40 and Aβ42 displayed aggregates through all the time points except fibrils were observed at 24 h for Aβ40 and at 4 h for Aβ42 (Figures 7 and 8). DMSO and HFIP treatment did not affect the aggregate formation of Aβ40 or Aβ42, nor did low-speed centrifugation (Figures 9 and 10).

The N-terminal modification of Aβ with fluorescein might also affect the ability of the peptide to form aggregates; hence, TEM studies were performed on F-Aβ40 and F-Aβ39E22Δ. Enhanced aggregates and/or fibrils were observed at baseline for both peptides (Figure 11), which further indicate that the species involved for binding to neurons is predominantly either early stage nonfibrillar or, in the case of Aβ39E22Δ, fibrillar aggregates. Similar experiments were conducted using AFM.

dx.doi.org/10.1021/bi300275g | *Biochemistry* 2012, 51, 3993–4003

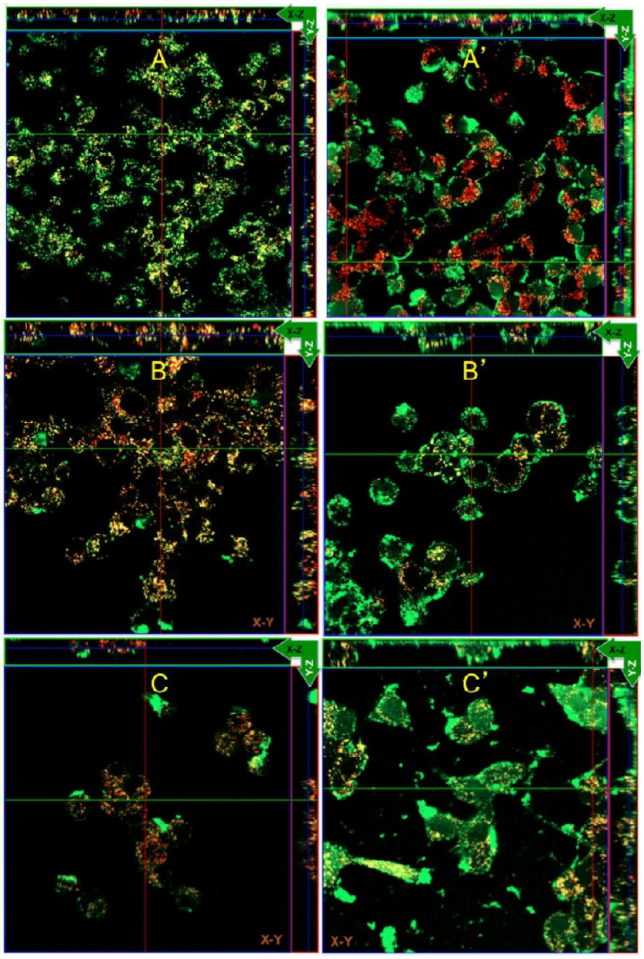

Figure 14. Accumulation of fluorescein-labeled Aβ40 (F-Aβ40) and Aβ39E22Δ (F-Aβ39E22Δ) and fibrils in the acidic compartments (labeled by Lysotracker Red) established by the *XY*, *XZ*, and *YZ* projections of differentiated PC12 cells: (A) uptake of F-Aβ40 peptide, (A′) uptake of F-Aβ39E22Δ peptide, (B) uptake of F-Aβ40 fibrils, (B′) uptake of F-Aβ39E22Δ fibrils, (C) uptake of sonicated F-Aβ40 fibrils, and (C′) uptake of sonicated F-Aβ39E22Δ fibrils.

Aβ39E22Δ showed predominantly aggregates with some beginning fibril formation at baseline; however, extensive fibrils were observed at 1 h (Figure 12). F-Aβ39E22Δ showed more extensive fibril formation at baseline with more mature fibrils at 1 h, which confirms the TEM studies indicating the N-terminal modification of the peptide did not affect subsequent aggregate/fibril formation (Figure 12). Again these studies confirm that fibrillar aggregates of Aβ39E22Δ are the major species involved in neuronal internalization that occurs during the 1 h incubation with PC12 neurons. Surprisingly, Aβ39E22Δ fibrils formed after a 7 day incubation showed levels of internalization by PC12 neurons comparable to those of fibrils formed after incubation for only 1 h (Figure 13). Lysotracker Red revealed both F-Aβ40 and F-Aβ39E22Δ colocalization in lysosomes (Figure 14). F-Aβ40 or F-Aβ39E22Δ fibrils with or without sonication also showed detectable accumulation in lysosomes with the deletion showing enhanced cell membrane binding. Time course studies are planned to further evaluate the intraneuronal distribution of these peptides and fibrils. Such Aβ fibril internalization by neurons has important pathophysiological implications for AD neurodegeneration that result from such intraneuronal Aβ accumulation.

TEM studies performed by Cloe et al.[12] revealed that Aβ39E22Δ formed numerous abundant fibrils that were more matted and twisted and had a smaller diameter than Aβ40. Ovchinnikova et al.[11] also observed that Aβ39E22Δ formed large networks of fibrillar bundles. It is apparent from our studies that the fibril structure varies among the different peptides as does the appearance of the aggregates. All the peptides formed an early stage aggregate, and the rate of transition from aggregates to fibrils was highly variable, with Aβ39E22Δ making the transition more rapidly than the other peptides. The extent to which these aggregates represent soluble oligomers is not clear and will require further evaluation with other techniques, such as size-exclusion chromatography, light scattering, etc. In any case, these differences in the rate of transition from aggregates to fibrils are thought to play an important role in the binding and internalization of these peptides by neurons, which in turn suggests that multiple pathways are involved depending on the aggregation/fibril state of the peptide.

Protein aggregate binding and internalization by cells is not without precedent. Ren et al.[14] reported that fibrillar polyglutamate peptide aggregates were internalized by mammalian cells where they accessed the cytoplasm to cosequester in aggresomes with the ubiquitin−proteasome and cytoplasmic chaperones. In addition, extracellular Tau aggregates, but not monomers, were demonstrated to be taken up by cultured cells.[15] These internalized Tau aggregates were shown to displace tubulin, colocalize with a marker of fluid phase endocytosis, and induce fibrillization of intracellular full-length Tau. Extracellular Tau aggregates, therefore, are capable of being transmitted as a misfolded state from the outside to the inside of a cell as well as between cocultured cells. The ability of an aggregated protein or fibril to cross a membrane barrier to access the cytoplasmic compartment has important implications for not only Alzheimer's disease but also for other neurodegenerative diseases associated with protein misfolding and amyloid production.

AUTHOR INFORMATION

Corresponding Author

*Mayo Clinic, 200 First Street SW, Rochester, MN 55905. Phone: (507) 284-1780. Fax: (507) 284-3383. E-mail: poduslo.joseph@mayo.edu.

Present Address

[§]Ph.D. program in chemistry at the University of California, San Francisco, CA 94143.

Funding

N.C.O. was a Summer Undergraduate Research Fellow (SURF) at Mayo Clinic while majoring in Biochemistry at California Polytechnic State University.

Notes

The authors declare no competing financial interest.

ABBREVIATIONS

Aβ, amyloid β-protein; AD, Alzheimer's disease; AFM, atomic force microscopy; Asp, aspartic acid; DMEM, Dulbecco's modified Eagle's medium; DMSO, dimethyl sulfoxide; DPBS, Dulbecco's phosphate-buffered saline; E22Δ, glutamate 22 deletion; F-Aβ, fluorescein-modified Aβ; HBSS, Hank's Balanced Salt Solution; HFIP, hexafluoro-2-propanol; TEM, transmission electron microscopy; TFA, trifluoroacetic acid.

REFERENCES

(1) Echeverria, V., and Cuello, A. C. (2002) Intracellular A-β amyloid, a sign for worse things to come? *Mol. Neurobiol. 26*, 299−316.

(2) Tseng, B. P., Kitazawa, M., and LaFerla, F. M. (2004) Amyloid β-peptide: The inside story. *Curr. Alzheimer Res. 1*, 231−239.

(3) Wirths, O., Multhaup, G., and Bayer, T. A. (2004) A modified β-amyloid hypothesis: Intraneuronal accumulation of the β-amyloid peptide—the first step of a fatal cascade. *J. Neurochem. 91*, 513−520.

(4) Gouras, G. K., Almeida, C. G., and Takahashi, R. H. (2005) Intraneuronal Aβ accumulation and origin of plaques in Alzheimer's disease. *Neurobiol. Aging 26*, 1235−1244.

(5) Li, M., Chen, L., Lee, D. H., Yu, L. C., and Zhang, Y. (2007) The role of intracellular amyloid β in Alzheimer's disease. *Prog. Neurobiol. 83*, 131−139.

(6) Kandimalla, K. K., Scott, O. G., Fulzele, S., Davidson, M. W., and Poduslo, J. F. (2009) Mechanism of neuronal versus endothelial cell uptake of Alzheimer's disease amyloid β protein. *PLoS One 4*, e4627.

(7) Poduslo, J. F., Gilles, E. J., Ramakrishnan, M., Howell, K. G., Wengenack, T. M., Curran, G. L., and Kandimalla, K. K. (2010) HH domain of Alzheimer's disease Aβ provides structural basis for neuronal binding in PC12 and mouse cortical/hippocampal neurons. *PLoS One 5*, e8813.

(8) Tomiyama, T., Nagata, T., Shimada, H., Teraoka, R., Fukushima, A., Kanemitsu, H., Takuma, H., Kuwano, R., Imagawa, M., Ataka, S., Wada, Y., Yoshioka, E., Nishizaki, T., Watanabe, Y., and Mori, H. (2008) A new amyloid β variant favoring oligomerization in Alzheimer's-type dementia. *Ann. Neurol. 63*, 377−387.

(9) Nishitsuji, K., Tomiyama, T., Ishibashi, K., Ito, K., Teraoka, R., Lambert, M. P., Klein, W. L., and Mori, H. (2009) The E693Δ mutation in amyloid precursor protein increases intracellular accumulation of amyloid β oligomers and causes endoplasmic reticulum stress-induced apoptosis in cultured cells. *Am. J. Pathol. 174*, 957−969.

(10) Tomiyama, T., Matsuyama, S., Iso, H., Umeda, T., Takuma, H., Ohnishi, K., Ishibashi, K., Teraoka, R., Sakama, N., Yamashita, T., Nishitsuji, K., Ito, K., Shimada, H., Lambert, M. P., Klein, W. L., and Mori, H. (2010) A mouse model of amyloid β oligomers: Their contribution to synaptic alteration, abnormal tau phosphorylation, glial activation, and neuronal loss in vivo. *J. Neurosci. 30*, 4845−4856.

(11) Ovchinnikova, O. Y., Finder, V. H., Vodopivec, I., Nitsch, R. M., and Glockshuber, R. (2011) The Osaka FAD mutation E22Δ leads to the formation of a previously unknown type of amyloid β fibrils and modulates Aβ neurotoxicity. *J. Mol. Biol. 408*, 780−791.

(12) Cloe, A. L., Orgel, J. P., Sachleben, J. R., Tycko, R., and Meredith, S. C. (2011) The Japanese mutant Aβ (ΔE22-Aβ(1−39)) forms fibrils instantaneously, with low-thioflavin T fluorescence: seeding of wild-type Aβ(1−40) into atypical fibrils by ΔE22-Aβ(1−39). *Biochemistry 50*, 2026−2039.

(13) Lakowicz, J. R. (1983) in *Principles of Fluorescence Spectroscopy*, Chapter 5, Plenum Press, New York.

(14) Ren, P. H., Lauckner, J. E., Kachirskaia, I., Heuser, J. E., Melki, R., and Kopito, R. R. (2009) Cytoplasmic penetration and persistent infection of mammalian cells by polyglutamine aggregates. *Nat. Cell Biol. 11*, 219−225.

(15) Frost, B., Jacks, R. L., and Diamond, M. I. (2009) Propagation of tau misfolding from the outside to the inside of a cell. *J. Biol. Chem. 284*, 12845−12852.